SECTION 4

ENERGY

GENERATION & CONVERSION

EXPERIMENTAL ANALYSIS OF DOWNDRAFT GASIFIER

Gerardo Flores
Justin Rine
Undergraduate Students
Department of Mechanical Engineering
West Virginia University Institute of Technology
Montgomery, WV USA

Farshid Zabihian
Department of Mechanical Engineering
West Virginia University Institute of Technology
Montgomery, WV USA

ABSTRACT

During times of emergency were gasoline shortages are likely to occur, gasoline has to be replaced by another suitable source of fuel. A downdraft gasifier is a piece of equipment used to turn solid carbon based materials into a gaseous fuel to run a spark ignition internal combustion engines. It is important to know that any kind of solid carbon based material can be used in the gasifier, but some materials work better than others, at the same time some materials are not found in a particular area. The most suitable source of carbon based material is to be found for the state of West Virginia. The construction of a gasifier is simple and is the most important part of this experiment. The gasifier used in this experiment was constructed in a similar manner as the one suggested by FEMA. Some of the parts were modified and some were added, but the most important addition was a water tank. The water tank will filter out solid impurities from the water and create hydrogen shift reaction giving the gas more combustibility. Some of the parts have to be constructed according to the size of the engine used. The carbon based materials are then to be chosen. The gasifier is run for 30 minutes at a time recording how much material was consumed. Several materials where tested and as expected some materials work better than others. Some of the reasons to why the variation on the amount of gas produced may be because of its composition and the amount of moisture in the material. Also some of the variation may happen because some of the materials are harder to fully catch fire and keep ignited than others. In conclusion, this experiment shows us what materials work best on a gasifier to produce alternative fuel source for a combustion engine. Most of these carbon based materials can be found in nature. At the same time the fabrication of the gasifier is inexpensive and the parts can be made out of recycled materials. Gasifiers are one of the best and least expensive alternatives for gasoline in times of crisis.

INTRODUCTION

The downdraft gasifier is a piece of equipment used to turn carbon based materials such as wood chips, coal, and corn cobs into a fuel that can be used to run a spark ignition internal combustion engine [1]. The fuel can also be used to heat an area or fuel a stove. The experimental analysis of the gasifier and fabrication has been completed and will be summarized below. During the experiment several different fuels were used to find which fuel type would give off the most burnable fuel with the least amount of the original fuel source being consumed.

The stratified downdraft gasifier was created for use during times of petroleum shortages. This device would be used on such cases as a prolonged war in which the petroleum reserves where used for military action and not readily available to the public or during times of natural disaster that left parts of the country or the whole country with a gasoline shortage. The gasifier would be a great secondary source of fuel for internal spark combustion engines since it can take several different sources of fuel and convert them into a gas to use [1, 2].

FABRICATION OF THE GASIFIER

A. Objective

The main objective of a downdraft gasifier is to turn a carbon based fuel source such as wood chips into a useable gaseous fuel for a spark ignition internal combustion engine. The gasification process happens due to the incomplete combustion of the carbon based fuel source. The incomplete combustion can be produced when the oxygen consumed in the combustion process is limited to allow the gas that is naturally produced from burning carbon based materials to be pulled through the system and burned at the end in either an internal combustion engine or burner.

B. Fabrication

The fabrication of the gasifier is the first part of the experiment. The complete unit is composed of several main pieces including the gasifier unit, filter/water unit, blower, and burner. Some of the parts were modified and some were added. The most important addition was a water tank. The water tank filters out solid impurities from the water and create hydrogen shift reaction giving the gas more combustibility [3]. Figure 1 illustrates the schematic diagram of a typical stratified

downdraft gasifier proposed by FEMA and Figure 2 shows the schematic diagram of the gasifier fabricated for this experiment. The main piece is the gasifier unit. The body of the gasifier unit is constructed from the body of a meat smoker. The fire tube and the bottom of the unit are constructed from duct work that was available. The hopper portion and the lower portion of the gasifier unit are separated by a round piece of steel. The fire tube was made to the specifications the FEMA outline Table 1 which was 6 inch diameter and 16 inches long. Some of components and the complete system can be seen in Figures 3 to 10.

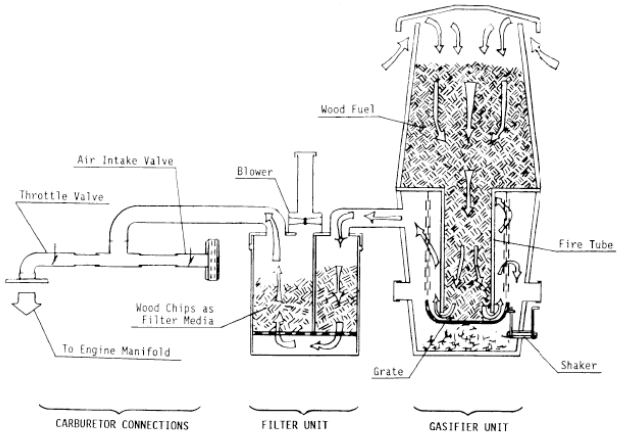

Figure 1. Schematic diagram of the FEMA stratified downdraft gasifier [4]

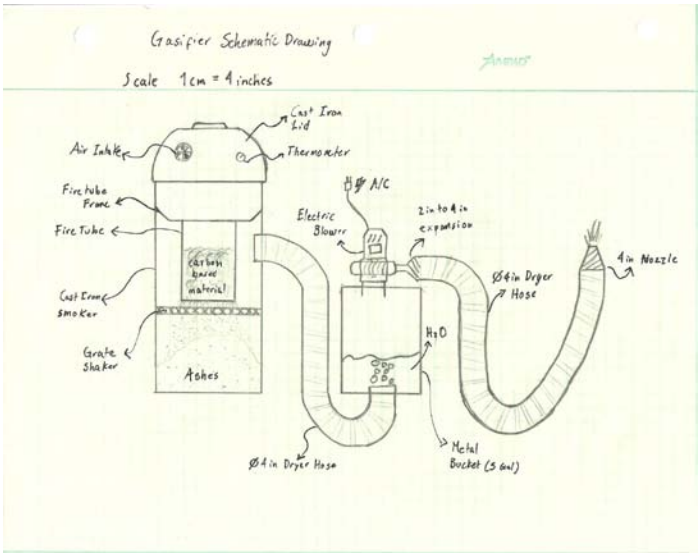

Figure 2. Schematic diagram of the fabricated gasifier

Table 1. The necessary size of the fire tube per hp rating of the engine [5]

Inside diameter (in)	Minimum length (in)	Engine power (hp)	Typical engine displacement (in^3)
2	16	5	10
4	16	15	30
6	16	30	60
7	18	40	80
8	20	50	100
9	22	65	130
10	24	80	160
11	26	100	200
12	28	120	240
13	30	140	280
14	32	160	320

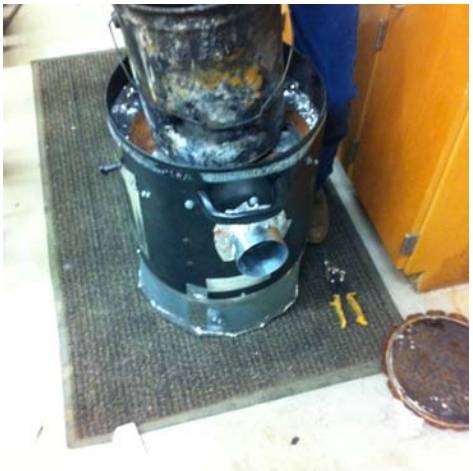

Figure 3. Construction of filter unit (five gallon bucket with outlet in bottom). The bottom part is the gasifier unit.

Figure 4. The inside of the filter unit (five gallon bucket) with dryer outlet attached. Inserted in the bottom and sealed with high temperature caulking.

Figure 5. Blower unit used to create the down draft inside the gasifier before it was incorporated into the system.

Figure 6. Blower unit attached to lid of filter unit.

Figure 7. The lid used to seal the filter system with dryer outlet inserted to hook up the blower unit. The unit is also sealed with high temperature caulking.

Figure 8. Completed gasifier unit connected to the filter system using dryer hose attached to two dryer outlets and sealed with metallic duct tape.

Figure 9. The completed gasifier unit before testing of fuel sources started.

Figure 10. Gasifier unit sitting outside while preparing for testing.

To seal all the seams and places where the gas could escape the system, metallic duct tape was used. Once the gasifier is lit, the smoker lid was placed on to limit the amount of air flow through the system. The filter/water unit was a metal five gallon bucket with a lid. To connect the gasifier to the filter/water unit a clothes dryer outlet was attached to the highest point in the bottom section of the gasifier and in the bottom of the five gallon bucket. Dryer hose was then connected and secured to the outlets. To seal the outlet in the bottom of the bucket a high temperature resistant silicone was used. The blower unit was connected to the lid of the bucket by a dryer outlet and sealed with silicon. A piece of dryer hose was then run from the outlet of the blower to a tip to burn the gas.

PERFORMING THE EXPERIMENTS AND RESULTS

The next step in the experiment is to select the fuel sources. Three fuel sources were chosen. These fuel sources where picked for their accessibility and ease of use. Wood chips, compressed wood pellets, and charcoal were chosen as the fuels for the experiment.

The experimental section of the project started with the testing of the different fuel sources. The experimental part was completed by measuring the amount of material used to run for a set time of 30 minutes. The first run was a test run. The air input, power of the blower and amount of water in the water unit were all adjusted to get the incomplete combustion and the combustion of the final product to occur. The first fuel source tested was the compressed wood pellets. The pellets burned for 30 minutes and at the end 1.2 pounds of pellets were burned. The second fuel source tested was the wood chips which yielded 30 minutes of burnable gas per 1.5 pounds of chips. The third source was charcoal. The charcoal yielded 30 minutes of burnable gas per 1.8 pounds. The amount of fuel used was measured by filling to a specific point before the 30 minutes of burning. The remainder left in the original bag of fuel source is weighed. The fuel is allowed to burn for 30 minutes then the hopper is filled back up with the amount of fuel source in the original bag then the amount in the original bag was weighed again. The amount used during the cycle was the difference in weight from the beginning weight of the bag and the end weight.

Figures 11 to 15 illustrate the various steps of the experiments.

CONCLUSION

The overall result was that the compressed wood pellets gave the best amount of material burned to time burned ratio. The reason for a gasifier to be produced and used would be in a case where there is a fuel shortage. Since these are mainly used in times of emergency most choices in material would be what is accessible in specific area. Out of the three that were tested

Figure 11. Smoke from the exhaust while starting the gasifier.

Figure 12. Smoke coming from the system exhaust while we were starting the fire in the fire tube.

Figure 13. Flame from burning the gasified fuel once a few minor modifications were made to the system to get the correct operation.

Figure 14. Top view of the fire inside the fire tube at the beginning before filling with the fuel source.

Figure 15. Top view of fire tube. Flame created if you do not turn the blower on to create the down draft.

here, the wood chips would be the most accessible source in times of emergency. The wood pellets and charcoal would need to be picked up from the store and in times of emergency these would most likely be inaccessible. Another factor would be the cost of the original fuel source. The wood chips would be the cheapest followed by the compressed wood pellets then the charcoal. So if money and accessibility is not limited, the best fuel to use from the three above would be the compressed wood pellets.

The experiment was conducted by fabricating a stratified downdraft gasifier and testing three different fuel sources. The amount of fuel used for a set run time was calculated for each

fuel then the results where compared and the most efficient fuel was found.

Some of the reasons to why the variation on the amount of gas produced may be because of its composition and the amount of moisture in the material. Also some of the variation may happen because some of the materials are harder to fully catch fire and keep ignited than others. In conclusion this experiment shows us what materials work best on a gasifier to produce alternative fuel source for a combustion engine. Most of these carbon based materials can be found in nature. At the same time the fabrication of the gasifier is inexpensive and the parts can be made out of recycled materials. Gasifiers are one of the best and least expensive alternatives for gasoline in times of crisis.

REFERENCES

[1] L AF Ontaine, H., and F. P. Zimmerman,. "Construction of a Simplified Wood Gas Generat or for Fueling Internal Combustion Engine S in a Petroleum Emergency." Soilandhealth.org. Federal Emergency Managment Agency, Mar. 1989. Web. 18 Sept. 2013.

[2] Milne, Thomas, Dr., and Thomas McGowan, Dr. "A Division of Midwest Research Institute Operated for the U.S. Department of Energy Handbook of Biomass Downdraft Gasifier Engine Systems." Nrel.gov. U.S. Department of Energy, Mar. 1988. Web. 12 Sept. 2013

[3] "CO Shift Conversion." - Process Plants Hydrogen and Synthesis Gas Plants Gas Generation. N.p., n.d. Web. 30 Sept. 2013.

[4] woodgasifier.webs.com

[5] driveonwood.com

Proceedings of the Fourteenth Annual Early Career Technical Conference
The University of Alabama, Birmingham ECTC 2014
November 1 – 2, 2014 - Birmingham, Alabama USA

GEOTHERMAL HEATING AND COOLING FROM ABANDONED COAL MINES IN WEST VIRGINIA

Jacob D. Bowen
Undergraduate Students
Department of Mechanical Engineering
West Virginia University Institute of Technology
Montgomery, WV, USA

Farshid Zabihian
Department of Mechanical Engineering
West Virginia University Institute of Technology
Montgomery, WV, USA

ABSTRACT

Heat pumps are a common alternative to a furnace and an air conditioner for heating and cooling homes across the United States. A typical air source heat pump uses the ambient outside air as a heat source and sink in heating and cooling a household. In contrast, the geothermal or ground-source heat pump introduced in this paper uses the constant temperature of the earth coupled with a ground-loop system as the heat source and sink, thus producing the same heating and cooling at a much more efficient rate than that of an air-source heat pump. This paper introduces a relatively different approach to burying the ground loop system by using abandoned coal mine shafts as a more economical alternative in West Virginia.

Keywords— Heat Pump; Abandoned Coal Mine; Geothermal; Residential Heating and Cooling.

INTRODUCTION

The United States Census Bureau concluded in 2012 that the State of West Virginia has a poverty rate of 17.5 percent. This number is higher than the average poverty rate in the United States of 14.3 percent. West Virginia also has a median household income of $39,550 compared to the national average $52,762 [1]. There are an abundance of sustainable and environmentally friendly resources these people can use, but many of them may not have the means or even the understanding to access and use them. The purpose of this research is to help those people living in poverty live a greener, more sustainable life and to do so in a more economical way and thereby lower their monthly electric or natural gas bills. The most expensive monthly utilities within a typical household are heating and cooling [2].

Throughout the state of West Virginia, there are a lot of abandoned coal mines. Many towns are near these abandoned mines and could possibly use them as a source for their heating and cooling. The temperature of the earth is around 55 degrees F year round and will be much more efficient than the outside air temperature as a source for heating or cooling using a ground source heat pump (GSHP) [3].

In the Morris Creek Water Shed outside of the town of Montgomery, West Virginia, there was a mining town named Donwood. This town no longer exists but what is left in its wake are many abandoned coal mines that could be valuable sources for heating and cooling the many houses in the area. After working with the Morris Creek Water Shed Foundation, a home was identified in the area in which the owner was willing to let research be conducted. The home, pictured below, is a 16 by 80 foot mobile home, located in close proximity to an abandoned coal mine shaft. This mine shaft is not flooded, but there are two other mine shafts that have a steady outflow of water. These locations are at what the watershed association calls the upper and lower main stems. At the upper main stem there is a constant outflow of 40 to 60 gallons per minute or more year round, while at the lower main stem there is a constant flow of at least 160 gallons per minute year round. Both of these mine drainages have a water temperature of around 54 degrees Fahrenheit. This makes these locations great places to install a geothermal heat pump system.

THEORY

The basic principles of a heat pump are very similar to an air conditioner. The only difference is that a heat pump can reverse its cycle to be used not only for cooling but also heating purposes. Below is a diagram of a heat pump to show how it works.

Figure 1: Mobile home near coal mine

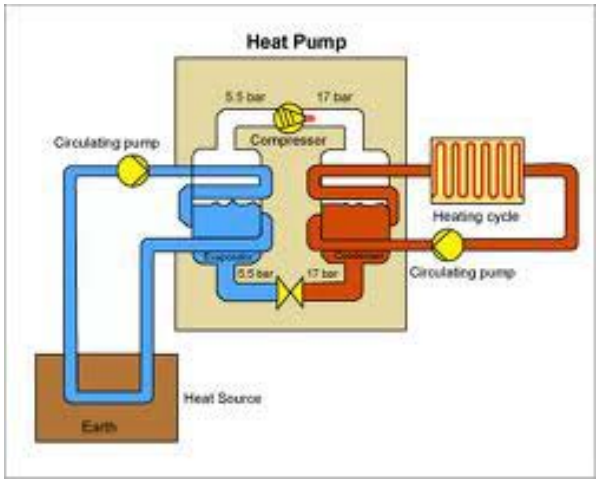

Figure 2: Schematic diagram of a heat pump [4]

The heat pump uses the refrigeration cycle much like an air conditioner, but the heat pump can reverse the cycle to heat or cool a home. The process begins with a refrigerant in an evaporator at an average temperature and low pressure that is compressed into a high temperature and pressure gas. From there, it goes through a condenser that condenses the high temperature vapor into a high temperature liquid. The liquid then goes through an expansion valve that cools the refrigerant to a low temperature before returning it to the evaporator. When a heat pump is used for heating, the cycle is run in the opposite direction, and the heat from the condenser is used to heat the house [5].

There can be toxic elements, such as carbon monoxide and many other dangerous elements inside an abandoned coal mine that would not be good to pump through a system that is heating a house. The safest way to use the heat from the mine is in what is called a closed loop system. This system uses a system of tubes or pipes that circulate the same fluid throughout the tubing as a medium to transfer the heat from the ground, or mine in this case, to the heat pump. Some systems use air that is circulated underground, while others use water from a well and discard the water elsewhere [6].

PROCEDURE

The first step in designing any heating and air conditioning system is to perform heating and cooling load calculations. In order to properly calculate the basic heating and cooling load of a structure, the dimensions and configuration of the outside of the structure must be measured. For example, a wall made of wood that has a double pane glass window must be divided into square feet of wood and square feet of window. The same procedure must be followed for the whole exterior of the house along with the formula below [7]:

$$Q = A \times U \times \Delta t \qquad \text{Equation 1}$$

A= Area of the surface
Q= Heat Transfer
U= Factor of material conductance
Δt= change in temperature from one side of surface to the other side

Once each heat transfer surface is calculated, the totals are added up to be the total heat transfer for the house given in units of BTU/hour [7].

Once the hand calculations were completed a numerical model was built using a software produced and made available freely online by the Canadian government. The software is called Hot2000 and is a home modeling software intended for use by home owners to help them understand what type of renovations can be done on their home to help increase sustainability and reduce electric consumption. After modeling the mobile home pictured above with a GSHP and an air source heat pump (ASHP), the heat load calculations done by hand were verified with the software. Also the consumption of electricity by the GSHP and the ASHP were compared. All of this data is tabulated below in the results section.

RESULTS

Tables 1 through 5 below compile the measurements, material properties, and hand calculated heat transfer values of the mobile home located in Montgomery, WV.

Table 1: Square footage of roof and floor

Length (ft)	Width (ft)	Square Footage (ft^2)
Roof		
80	8.25	660
80	8.25	660
Floor		
80	16	1280

Table 2: Square footage of windows and doors

Width (in)	Height (in)	Square feet (ft^2)
Windows		
30	41	8.54

30	28	5.83
30	55	11.45
30	55	11.45
30	41	8.54
30	41	8.54
30	41	8.54
16	41	4.55
30	55	11.45
30	55	11.45
Total		90.38
Doors		
34	76	17.94
34	76	17.94
Total		35.88

Table 3: Square footage of walls

Height (ft)	Width (ft)	Square Footage (ft^2)
9	80	720
9	80	720
9	16	144
9	16	144
Total		1,728

Table 4: Materials and U factor [4]

Material	U factor
Walls	0.55
Double pane windows	0.45
Door with glass storm door	0.38
Door	0.59
Roof	0.57
Floor	0.38

Table 5: Calculated heat transfer through surfaces

Material	Heat transfer (Btu/hr)
Windows	610.1
Doors	261.0
Walls	13,214.4
Floor	7,296.0
Roof	9,900.0

With a temperature difference of 15 degrees F, the total heat load calculation for this home sums up to be 31,281.5 Btu/hr. The data below was found from the Software Hot2000. The first set of data is from the ASHP and the second set of data is from being modeled with a GSHP. In the model of an air source heat pump in Hot2000 all of the following data tabulated below was found.

Table 5: Hot2000 heat pump results for comparison of ASHP and GSHP

System Type	Heat load (Btu/hr)	Annual Heating Energy (kwh)	Annual Cooling Energy (kwh)	Cost ($)
ASHP	33,500	10,668.7	7,412.5	1,988.9
GSHP	33,500	8,316.9	668.7	998.4

This data shows that the GSHP is 18.7 percent cheaper to operate than an ASHP. This model also helps to validate the hand calculation of the heating load.

Table 6: Hand calculations vs. Hot2000 model

Hand Calculation	Hot2000 Calculation	Percent Difference
31,281.5 BTU/hr	33,500 BTU/hr	6.8 %

The Hot2000 modeling software has some error the results it related to the inability to properly account for the crawl space under a mobile home that differentiates it from a conventional home.

Once the size of heat pump needed is calculated, the next step is to choose a heat pump to install based on the tonnage of load of the heat pump. To determine the tonnage of the heat pump, the BTU's/hour must be divided by 12,000. This gives the tonnage of heating and cooling needed. The tonnage required for this mobile home is 2.79 tons from the HOT2000 numbers and 2.606 tons for the hand calculated numbers. Due to the small size of the mobile home, a 2.5 ton unit was chosen for both the air source and ground source models.

The ground temperature within the software based on using the geographical location of the home and a depth underground at this location. The temperatures fluctuated from month to month in the range of 8 degrees Celsius and 15 degrees Celsius. Once the model was completed and the testing was ran performed, no significant difference was found in the cost of heating or cooling. The change was so slight that for cooling it

was found to be 18 dollars cheaper and for heating it was found to be 56 dollars cheaper.

. The costs of the installed GSHP and ASHP systems the cost of installations, and the annual operating costs are given in Table 7.

Table 7: Cost comparison GSHP and ASHP systems

System	Cost of System	Cost to Install System [10]	Annual Running Cost
GSHP	$6,702	$10,000	$998
ASHP	$3,179	$1,000	$1989

This cost calculation is based on a conventional installation, meaning that holes must be dug in a yard to install the ground loops. If the ground loops are installed within an existing mine shaft, it will reduce the installation costs associated with the ground loops significantly. Assuming that the cost of installation is roughly $2,000, and that the cost of digging is roughly 80 percent of installation costs [10], the GSHP system would have a3.5 year payback period.

EXTENDED ANALYSES IN HOT2000

Three separate parameters were evaluated and compared to the annual energy consumption of a manufactured house. This model was used to assure that the modeling process was done properly and that the only changes made were to the geothermal heating system. The depth of the pipes buried within the ground to absorb the geothermal energy was changed from 6 feet to 12 feet in 2 foot intervals and was compared to the annual kilowatt hour consumption of the heating ventilation and air conditioning (HVAC) system. The ground temperature was calculated by the software using the geographical location of the home. The results are shown below in Figure 3.

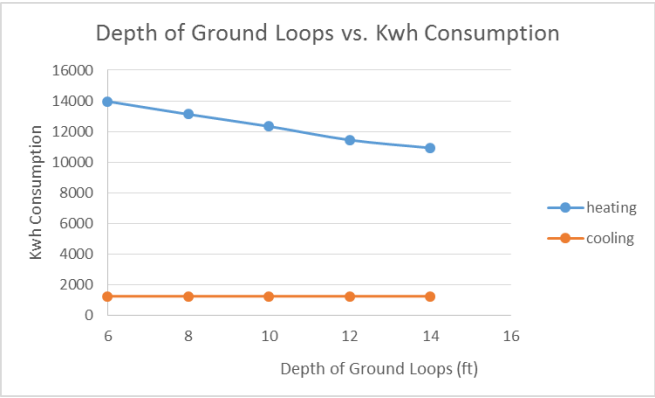

Figure 3: Depth of piping vs. annual energy consumption (kWh)

Next the depth of the piping was set at a depth of 6 feet and the ground temperature was set at a given temperature of 40 degree Fahrenheit and increased by increments of 5 degrees until 60 degrees was reached. This data was also compared to the annual kilowatt hour consumption of the HVAC system. Figure 4 shows this comparison.

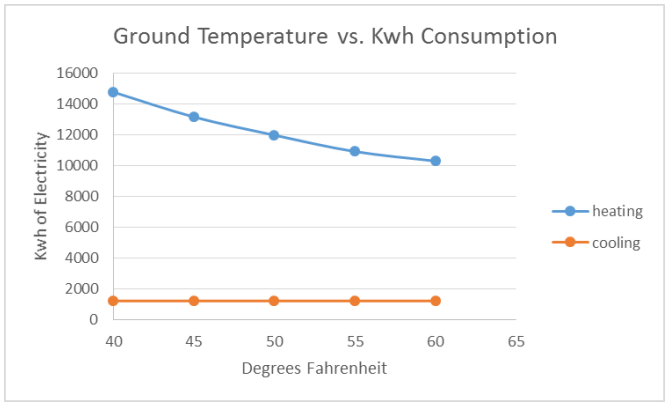

Figure 4: Ground temperature vs. annual energy consumption (kWh)

The final comparison made was to set the depth of the ground loop piping to 6 feet and let the software calculate the ground temperature while changing the coefficient of performance (COP) of the geothermal heat pump from 1 to 5 in increments of 1. The COP of an HVAC system is the ratio of heating or cooling provided compared to the energy consumed. This comparison is shown below in Figure 5.

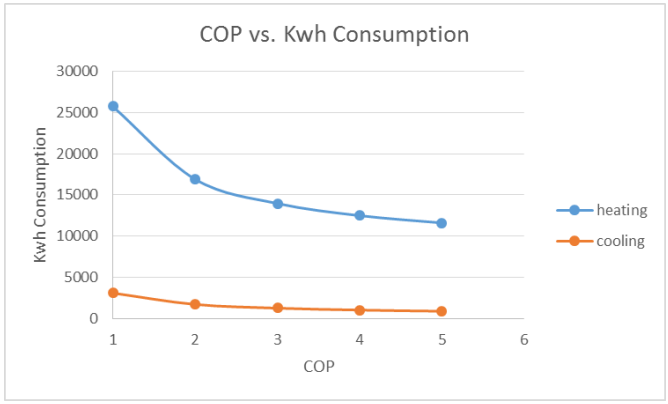

Figure 5: COP vs. annual energy consumption (kWh)

FUTURE RESEARCH POTENTIALS

The Morris Creek Watershed area has proven to be a great location for research within the field of geothermal technologies. Having two mine shafts with endless out flow of 54 degree Fahrenheit water year round is ideal case in this project. After discussing the possibilities of getting mine maps with the owner, new information has revealed that the lower main stem mine shafts go as far underground and beneath the town of Montgomery, WV. This could prove to be a great resource for the township to use as a source of low-grade geothermal energy for use within municipal buildings, schools, and even residential homes.

CONCLUSION

The research above shows that using different types of heating and cooling energy sources can reduce their cost of living and provide an essential set of utilities for low-income households. By using resources already in place, people can offset the costs of implementing the systems suggested within this paper. When looking at the saving that can come from using an abandoned mine shaft it can be seen a large reduction in cost and a large amount of savings over the course of 20 years. Modeling was performed to verify the economic impacts of using geothermal energy as a source to heat and cool one's home as well as the feasibility of using abandoned coal mine shafts as a source for this geothermal energy. It can be concluded that with access to a coal mine with a large enough outflow of water at the right temperature, individuals and families stand to benefit from using these old mines as a resource to offset the costs of heating and cooling of their home.

REFERENCES

[1] www.cesus.gov/

[2] Crowe, Aaron. 10 Most Costly Appliances. June 10, 2010. www.DailyFinance.com

[3] http://www.alliedwells.com/geothermal-martinsburg-wv

[4] http://sd-lt.en.alibaba.com/

[5] Sonntag, Richard. Borgnakke, Claus. *Fundamentals of Thermodynamics*. 7th. John Wiley & Sons, 2008. Print.

[6] Harvrella, Raymaond A. *Heating, Ventilation, and Air Conditioning Fundamentals*. Prentice Hall 1995. Print.

[7] 1989 ASHRAE Handbook

[8] www.ingramswaterandair.com

SOLAR SIMULATOR TEST OF WIRE MESH PARTICLE HEATING RECEIVER TO MEASURE RECEIVER EFFICIENCY

Matthew Golob, Clayton Nguyen, Robert Gill
Sheldon Jeter, Said Abdel-Khalik
Georgia Institute of Technology
Atlanta, Georgia, USA

ABSTRACT

Solar receiver technology is exploring new possibilities, particularly in pushing higher temperature ceilings to improve power cycle efficiency. This move has shifted solar receivers from troughs using heat transfer oils to central receivers utilizing molten salts that can capitalize on the higher concentration flux and resulting higher output temperature. While molten salts have allowed for high receiver temperatures, they are limited by cost and composition. The higher temperatures and potentially resulting higher efficiency can be reached by utilizing particulates instead. Particulates such as commercially available aluminia based products offer two key benefits. (1) Unlike typical molten salts which are restricted by phase changes to operating ranges between 240°C to 565°C [1], these ceramic particles are stable to over 1000°C [2] and ID-50K melt at 2200°C [3]. (2) While not a fluid, they can still be flowed through a structure allowing for much better heat exchange regimes.

To explore this alternative potential, an experimental trial at Georgia Tech has been developed to assess the efficiency and effectiveness of a heating receiver employing particles. The basic approach of the receiver is to drop particles vertically through the irradiated space in order to heat them. Instead of simply dropping the particles through the heated zone, a chevron wire mesh is employed in the receiver to slow the free fall of particles increasing residence time and temperature rise per fall length. The overall experiment uses a calibrated source of concentrated radiation from a solar simulator as the energy input and measure the energy collection from the temperature rise in a mass flow rate of particulate dropped through the test receiver. With a measured energy rise of the particulate and known energy input, the particle heating receiver efficiency can be calculated.

The results here are from preliminary data collected using a small scale receiver using the Georgia Tech Solar Simulator, which employs a bank of high intensity xenon lamps, as the simulated solar source. These results show a preliminary thermal efficiency of a small scale particle heating receiver to be around 90%.

1. INTRODUCTION

The experiment covered in this paper is an ongoing iteration of test receiver designs utilizing Georgia Tech's Solar Simulator (GTSS). What is learned here is used to support key components of a larger scale receiver design involving the Department of Energy's SunShot program. The GTSS consists of a bank of 7 xenon lamps all focused down to a point approximately 80 mm in diameter, Figure 1. This device serves as a convenient artificial concentrated solar irradiation source and can output concentration ratios well in excess of 1000 suns.

Figure 1. GTSS test of Focal Plane

Figure 2. Former recirculating OLDS elevator configuration

Improvements on the previous particle heating receiver (PHR) apparatus resulted in a switch from a recirculating OLDS elevator configuration, Figure 2, to a large single pass hopper particle system for better temperature stability and mass flow sensing. The previous setup also tested likely receiver designs, covering two receiver configurations: a simple free-falling curtain and a chevron wire-mesh design to inhibit free flow. These will be repeated and further studied. The GTSS has also undergone considerable improvements to correct some electrical issues as well as refinements in the operation, alignment, and focus of the lamps. As a result a more nearly uniform (but not perfect) hot spot can now be generated with about 80% of the incident radiation falling within an approximately 80 mm diameter circle. The updated apparatus can simulate the high fluxes expected in practical operations (~250 to as much as 2000 kW/m^2).

The new apparatus has been developed to provide a single-pass high-temperature transient test employing the GTSS. This apparatus consists of a 25.4 L supply hopper, which will have the option of pre-heating particles to around 300°C. The hopper is designed to deliver the particles at a fixed flow rate to the irradiated test receiver region located at the focus, Figure 3, thereby simulating operation of a small representative subset of a larger PHR. The flow rate is regulated utilizing a perforated plate which simultaneously disperses and controls the flow to prevent regional overloading in the receiver as well as ensuring a constant flow rate in the saturated state.

2. LITERATURE REVIEW

One purpose of the SunShot project is to explore and improve the particle heating receiver component of the solar concentrator power cycle. This is a relatively new field of research so there are a limited range of studies with which to compare.

Figure 3. Receiver Test Region

Previous research at SNL [4] has examined alternative receiver designs for a high efficiency particulate solar receiver. These designs feature a receiver cavity box with a free falling particulate curtain. Their work focused on varying the cavity depth, the ceiling slope angle, the specular properties of the walls and the back geometry in order to improve the efficiency of the solar receiver. In comparison to their base receiver design with a vertical aperture, the new design increases the theoretical thermal efficiency from 72.3% to 86.8%. SNL's work on the free falling curtain is a core PHR candidate for the SunShot program. The main drawback is the significant particle acceleration of the free fall setup, a downside of which the chevron mesh design seeks to eliminate.

Tan et al. [5] also looked at falling particle receivers. Their research mainly dealt with computational simulation of wind effects on the receiver. An aerowindow was a suggested addition to the aperture of solid particle solar receivers. The aerowindow acts as an air curtain which would help prevent the loss of heated air to the ambient conditions. In addition, it has the added advantage of ensuring particle retention. While noteworthy ideas, there is little here in terms of physical tests or measurements with which to compare receiver efficiencies against.

Xiao et al. [6] is perhaps one of the closest experiments to ours, mainly through the use of lamps and physical receiver. Zhejiang University used a similar Xenon-arc lamp bank as a solar simulator to test a spiral solid particle solar receiver. This receiver cavity resembled a sunken helical spiral and employed a top facing aperture with a glass window cover. The receiver was experimentally measured to achieve a temperature rise exceeding 350°C for a single pass with a 19.3 kW/m^2 focal flux off the lamps. The receiver had an optical efficiency of 84% and a thermal efficiency of 60%. The general setup is

somewhat similar to our test, although there are significant differences in receiver geometry, orientation, and particle flow regimes.

Röger et al. [7] looked at different Solid Particle Receiver (SPR) designs utilizing varying particle recirculation schemes in order to maximize the particle heating. The general particle recirculation schemes focused on increasing particle residence time to in turn increase the thermal efficiency of the receiver. While the studies do not rigorously account for convective losses, they did highlight the need to increase particle residence time in the receiver.

3. EXPERIMENTAL SETUP

The chevron mesh design to be tested is also similar to the inlet region of a falling curtain in terms of average particle fall speed. As an objective, the ultimate form of the system will be able to investigate high-temperature collection efficiency and provide empirical data to support detailed computer modeling. The basic design for the system can be seen in Figure 4. The cone of light shown in the image illustrates a representative inlet cone from the seven solar simulator lamps.

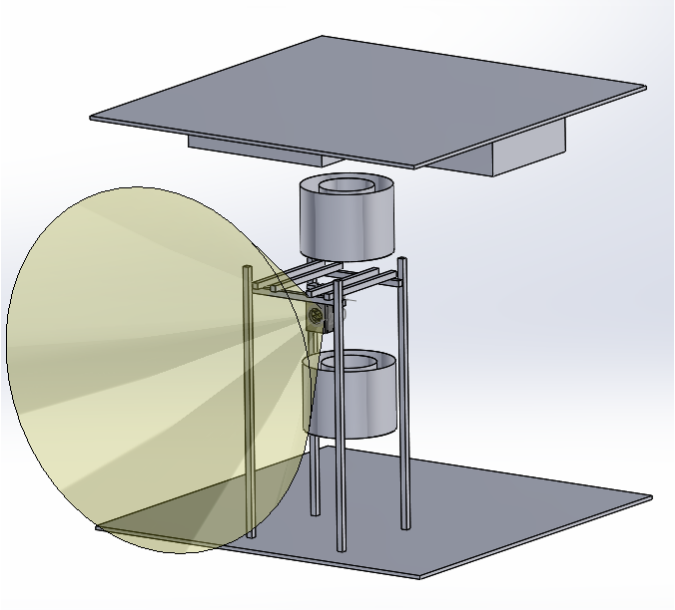

Figure 4. Single pass test apparatus

To determine the incident solar irradiation the GT SunShot Research Team has been assisting the GTSS operators in developing a water cooled cavity calorimeter, similar to the one produced by Groer and Neumann [8], to accurately measure the amount of concentrated radiation being delivered to the receiver. For the preliminary tests conducted on the single pass receiver, only a single lamp running at approximately 80% power was used. The GTSS team has been refining the solar simulator and the calorimeter to work with more lamps.

The calorimeter consists of a copper surface coated in high absorptivity black. When an iris plate is mounted to the front of the calorimeter, the core serves as a black body. The core is further swathed in insulation to minimize heat loss. The assembly is encased in a large steel pipe to provide support as well as mountings for the iris plate. Line water is run through copper tubing in the assembly with temperature taps taking the incoming and outgoing water stream measurements. A positive displacement flow meter is also located on the water line to gauge the water flow rate. The resulting heat inputs of the lamps are determined by the following equation.

$$\dot{Q}_{\text{Input}} = \dot{m}_{\text{w}} \cdot c_{p,\text{w}} \cdot \left(T_{\text{w,out}} - T_{\text{w,in}}\right) \qquad (1)$$

where $\dot{Q}_{\text{Input}}$ is the calculated heat rate from the lamp, $\dot{m}_w$ is the recorded flow rate of the line water, $c_{p,\text{w}}$ the specific heat of water, $T_{\text{w,out}}$ the measured outlet water temperature, and $T_{\text{w,in}}$ measured the inlet water temperature. In order to apply a lamp's heat rate to a different experimental setup, an image of a Lambertian target at the same focal plane as the calorimeter was taken. The intensity of the light recorded in the image was then calibrated to the measured heat rate for that plane at the diameter of the calorimeter iris. With this and a new image of the PHR as well as the new iris diameter on the receiver, an equivalent heat input rate could be correlated to the test wire mesh PHR. At this time the average of the best apparent image data and available calorimetry measurements gives a heat rate of 1.92 kW into the PHR from a single lamp. The research team has made plans to design a calorimeter that fits the exact aperture of the current test PHR to refine the heat rate assessment.

To test the PHR concept, a small scale receiver has been fabricated for testing in the Solar Simulator Lab. The receiver's back wall is 0.102 m by 0.203 m and acts as a representative portion of a larger receiver that will be used at SNL. The receiver space is filled with 10 mesh wire chevrons that slow the falling particles in the irradiated zone. The targeted focal plane is an inch off the back wall towards the receiver aperture. According to the GTSS team's simulator modeling, that spot should receive approximately 80% of the irradiative power provided by the lamps. The iris plate that covers the front of the receiver was built to allow the 80% portion of the light in while shielding rest of receiver from the remaining incident irradiation. This also protects the thermocouples in the receiver from any direct irradiative exposure.

The single-pass solar simulator is being tested using ID50-K particulates. The ID50-K is a primarily alumina comprised particulate [3] that has high absorptivity and is the candidate medium for the SunShot PHR. In order to run this test, a water-cooled Lambertian shield was placed in front of the receiver to protect it until the lamps reached steady state operation, Figure 5. A few seconds prior to the shield's retraction, the valve controlling the particulate flow would be opened to allow for ID50-K to start passing in a steady flow state through the receiver. This would begin a test run. The run ends when the top hopper is nearly exhausted.

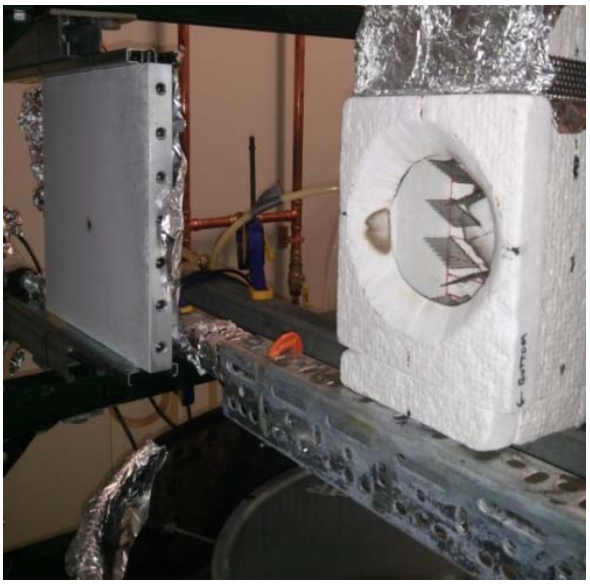

Figure 5. Solar simulator test receiver with water cooled shield

4. MEASUREMENTS

K-type Thermocouples with a ±2.2°C accuracy are placed into the inlet hopper to measure the particulate temperature as it enters the receiver. These thermocouples have similar readings at ambient temperatures (all within ±0.2°C) and have only been used for low temperature testing. In the future their accuracy will be increased through calibration to a Standardized Platinum RTD. Several more K-type thermocouples are set immediately downstream of the receiver focal point in an irradiative shielded particle flow catch to measure the exiting particle stream temperature. As testing proceeded it was discovered that a temperature gradient forms within the particulates making it difficult to measure a mixed temperature outlet. To compensate for this, two methods were employed to measure the outlet temperature.

The first was to place a series of nine thermocouples in a 3x3 grid in the irradiative shielded particle flow catch located just below the discharge of the receiver focal point. These 9 thermocouples gauge the temperature gradient, and are used as an unweighted average of the mass flow. Due to difficulties in forming the thermocouple array in such close proximity to each other only eight thermocouples were used in the preliminary measurements with the ninth accounted for via symmetry.

The problem with the thermocouples arises due to the two metal plates that are used as vanes as seen in Figure 6. These vanes attempt to alter flow in the hopes of creating a mixed flow catch. Unfortunately these plates cause significant flow shadowing and do not allow for some of the outer thermocouples to be well submerged. The center array of thermocouples provided values that remained consistent and stable. The left and right arrays were subject to inconsistencies and fluctuation due to small perturbations in in flow coming off the vanes. The solution will be to replace these vanes with a mesh vane setup allowing the flow to be more evenly distributed into the bead locations. Overall though, there were portions of the runs were the outer thermocouples were stable enough for a tentative reading.

The efficiency of the receiver was calculated by comparing the assessed input heat rate from the lamp, $\dot{Q}_{\mathrm{Input}}$, to the measured heat rate gain seen in the particulates, $\dot{Q}_{\mathrm{Part}}$.

$$\dot{Q}_{\mathrm{Part}} = \dot{m}_{\mathrm{p}} \cdot c_{p,\mathrm{p}} \cdot \left(T_{\mathrm{p,out}} - T_{\mathrm{p,in}}\right) \quad (2)$$

The heat rate gain of the particulate is calculated by, $\dot{m}_{\mathrm{p}}$, which is measured mass flow rate of the particulate into the base hopper, $c_{p,\mathrm{p}}$, the specific heat of ID-50K, $T_{\mathrm{p,out}}$, the average mixed stream temperature at the receiver discharge or mixed hopper temperate, and $T_{\mathrm{p,in}}$, the average incoming particulate stream temperature from the top hopper. The resulting efficiency is calculated by equation 3.

$$\eta_{\mathrm{r}} = \frac{\dot{Q}_{\mathrm{Part}}}{\dot{Q}_{\mathrm{Input}}} \quad (3)$$

where the calculated receiver efficiency is the heat rate gain of the particulate divided by the heat input rate from the lamp.

Figure 6. Flow test through the receiver

Using the temperatures recorded at the inlet and exit of the receiver, the receiver efficiency was transiently calculated. As shown in Figure 7, once the receiver reaches a steady state the average receiver efficiency is 90.8%. The initial disturbance in the efficiency at about 600 seconds is due to a slight blockage in the discharge creating a onetime change in the mass flow rate.

The other measurement method employed immediately mixing the resulting mass of particulates in the catch hopper using a hand-drill powered mud mixer upon the runs conclusion. This time consuming mixing process did have a significant heat loss but provided a meaningful mixed particulate temperature that can provide a reasonable baseline value for the receiver efficiency. To measure the mixed particulate bulk in the hopper, a K-type temperature probe was

inserted the same depth at each location. Once the temperature had stabilized the temperature was recorded as shown in

Figure 8. The average temperature of the hopper was 42.9°C and results in a receiver efficiency of 91.8%.

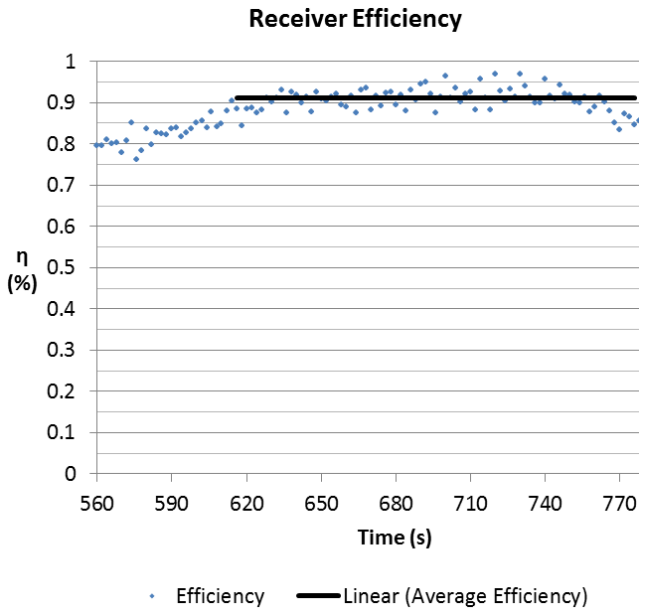

Figure 7. Receiver efficiency with averaged TC grid, a steady state efficiency of 90.8% from 620s to 770s

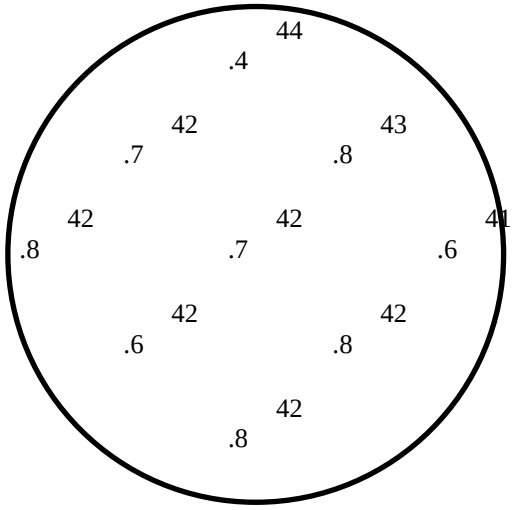

Figure 8. Temperature (°C) of the particulates at varying locations in the bottom hopper

5. CONCLUSION

The preliminary results of the test show that the discrete structure receiver using a size 10 mesh can potentially achieve receiver efficiency greater than 90%. However, the tests also show that the thermocouples must be fine-tuned both in placement and calibration in order to better capture the dynamic flow conditions. In addition a more active mixing protocol must be investigated to get a better average receiver discharge temperature for the particles. Another key item will be the fabrication of a calorimeter tailored to more effectively gauge the incoming lamp flux based on the current test receiver geometry. With these changes, upcoming tests will further focus on repeating runs at elevated temperatures and comparing runs with altered mesh layouts as well as a free falling configuration. Overall these measurements will determine the PHR efficiency over a range of conditions and guide the design path of the SunShot's large scale PHR.

Nomenclature

PHR	Particle Heating Receiver
SNL	Sandia National Laboratories
GTSS	Georgia Tech Solar Simulator
SPR	Solid Particle Receiver
$\dot{Q}_{\text{Input}}$	Heat rate input from lamp
$\dot{m}_{\text{w}}$	Water mass flow rate
$c_{p,\text{w}}$	Specific heat of water
$T_{\text{w,out}}$	Calorimeter outlet water temperature
$T_{\text{w,in}}$	Calorimeter inlet water temperature
RTD	Resistance Temperature Detector
$\dot{Q}_{\text{Part}}$	Heat rate gain of particulate
$\dot{m}_{\text{p}}$	Particulate mass flow rate
$c_{p,\text{p}}$	Specific heat of Accucast ID-50K
$T_{\text{p,out}}$	Receiver outlet particulate temperature
$T_{\text{p,in}}$	Receiver inlet particulate temperature
η_{r}	Receiver efficiency

ACKNOWLEDGMENT

Financial support of the US Department of Energy through the SunShot research program is recognized and appreciated.

REFERENCES

[1] Ortega, J., Burgaleta, J., Téllez, F., 2008, "Central receiver system solar power plant using molten salt as heat transfer fluid", *Transactions of the ASME, 2008, Journal of Solar Energy Engineering*, 130.

[2] Hruby, J. M., 1986, "A Technical Feasibility Study of a Solid Particle Solar Central Receiver for High Temperature Applications," SAND87-8005, 1986, Sandia National Laboratories Albuquerque, NM

[3] "CarboAccucast ID-50K", Carbo Ceramics, 2014, Houston, TX, www.carboceramics.com

[4] Christian, J., Ho, C.K., 2013, "Alternative Designs of a High Efficiency, North-facing, Solid Particle Receiver", *SolarPACES 2013, Energy Procedia 49 (2014) pg. 314-324, doi: 10.1016/j.egypro.2014.03.034*

[5] Tan, T., Chen, Y., Chen, Z., Siegal, N., Kolb, G., 2009, "Wind effect on the performance of solid particle solar receivers with and without the protection of an

aerowindow", *Solar Energy, Oct. 2009, Vol. 83, pg. 1815-1827*
[6] Xiao, G., Guo, K., Luo, Z., Ni, M., Zhang, Y., Wang, C., 2014, "Simulation and experimental study on a spiral solid particle solar receiver", *Applied Energy, Jan. 2014, Vol. 113, pg. 178-188*
[7] Roger, M., Amsbeck, L., Gobereit, B., Reiner, B., 2011, "Face-Down Solid Particle Receiver Using Recirculation", *Journal of Solar Energy, July 2011, Vol. 133, doi:10.1115/1.4004269*
[8] Groer, U., and Neumann, A., 1999, "Development and test of a high flux calorimeter at DLR Cologne," *Journal De Physique. IV: JP, 9(3), pp. Pr3-643 - Pr643-648.*

Proceedings of the Fourteenth Annual Early Career Technical Conference
The University of Alabama, Birmingham ECTC 2014
November 1 – 2, 2014 - Birmingham, Alabama USA

APPLICATION OF VERTICAL AXIS WIND TURBINES IN WEST VIRGINIA

Alex Perry
Tavon Johnson
Andrew Thaxton
Undergraduate Students
Department of Mechanical Engineering
West Virginia University Institute of Technology
Montgomery, WV USA

Farshid Zabihian
Department of Mechanical Engineering
West Virginia University Institute of Technology
Montgomery, WV USA

ABSTRACT

This project was initiated to study the effects of West Virginia's topography on wind energy and how Vertical Axis Wind Turbine (VAWT) could be utilized to harness energy that may otherwise be lost by conventional horizontal axis turbine designs. This would cut down West Virginia's dependence on non-renewable energy, and create a path to a sustainable energy for the future of the state. As fossil fuels continue to be regulated and reduced, sustainable green energy will be key to the future of the state.

The study was conducted by examining topographic maps, wind direction maps, and field research. By observing the direction that wind flows in West Virginia, it was easy to see why conventional turbines could not be used in majority of West Virginia's counties. It was apparent that the most powerful wind is found along the eastern boarder of West Virginia. At a higher elevation wind becomes very turbulent, which is mainly due to the wind deflecting off of higher mountain peaks to the east. Because of the design of the VAWT, its rotors can receive wind velocity from any direction; this makes it good for mountainous regions.

Through the research presented in this report, it has been determined that to some extent, VAWTs are underestimated in urban regions.

Keywords— Vertical Axis Wind Turbine; VAWT; West Virginia

INTRODUCTION

The objective of this study was to determine whether VAWTs could increase energy output in the state of West Virginia. This study was intended to show that due to the states varying topography, wind patterns are turbulent in the majority of the state. Conventional wind turbines with horizontal axis rotors would be rendered useless in these cases because the rotor blades must be facing the direction of the wind [1]. If the wind was to shift, the turbine must be rotated to receive the wind in a different direction, which limits its efficiency [1]. VAWTs are wind mills that use vertical axis rotors to catch wind [3]. Due to their design, they tend to be more dependable than conventional horizontal axis turbines [3]. The cost of VAWTs tend to be lower than conventional designs in most cases [3]. Wind patterns in the eastern part of the state are very unpredictable, especially in valleys, where wind patterns could change by the minute [2]. VAWT systems are able to adjust to changing wind directions, unlike conventional Horizontal Axis Wind Turbines (HAWT).

The Savonious VAWT is the most crude, simple version of a VAWT. It is drag based, and is usually composed of cheap materials [4]. It is generally the least expensive version, and has an efficiency output proportional to its value [4].

Darrius VAWTs tend to be the most effective type of the VAWT designs [5]. It allows for the turbine to stall more efficiently when a large gust of wind targets the vertical rotors [5]. This design technique allows for the turbines to be more tightly packed, because horizontal turbines essentially slow the wind around them down, while vertical axis turbines do not disrupt air flow as much [5]. Although there are some VAWTs with rotating vertical rotors, they have never been made on large scales due to complications with their necks, which tend to fracture easily [5]. According to a study done by a group of private researchers in Italy, Darrieus VAWTs are much more effective when on roofs of buildings or on top of mountains as opposed to when they are on the ground [6]. In this study, efficiency maxed out at 70%, whereas energy production in

the same conditions when the turbines were on the ground was much lower, at about 43% to 49% [6].

The third major VAWT design is the H-Rotor. The design of this turbine is similar to that of a Darrieus turbine, but with the modification that the mill blades are parallel to the horizontal axis of the turbine [4].

VAWTs have many benefits; they require less wind to generate power, and are far quieter than conventional wind turbines [5]. According to studies, VAWT increase energy output significantly [3].

In many early cases, VAWTs had problems with the central shaft cracking due to stress exerted by the rotors [3]. Also, in some cases, after successfully stalling to prevent wind damage due to large gusts of wind, they occasionally have trouble starting back up again [1]. However, today VAWTs do not encounter these problems because they have been resolved by the ever-popular Darrius design. Despite being stereotypically viewed as inefficient, VAWT farms have become more popular worldwide. VAWTs also tend to cost far less than horizontal wind turbines; repair and maintenance costs are lower in spite of cracking in central shafts [1].

RESULTS

Due to the VAWTs ability to pick up wind coming from any direction, it is more lucrative in rough terrain as opposed to horizontal axis wind turbines [7]. VAWTs are mainly attractive to small buisnesses and individuals who will use them for low power consumption [8]. Some charachteristics that make VAWTs attractive are that they are generally small, short and quiet [6].

From this research, it was determined that much of West Virginia has a very rough topography. Mountains, hills and valleys make up most of the landscape of West Virginia. Figure 1 shows a topographic map of the state, which shows that the terrain becomes less mountainous in the western portion of the state [9].

Figure 1: West Virginia topographic map [9]

Figure 2 shows an elevation map of West Virginia [9]. This map shows that the highest elevations are in the eastern part of the state [9].

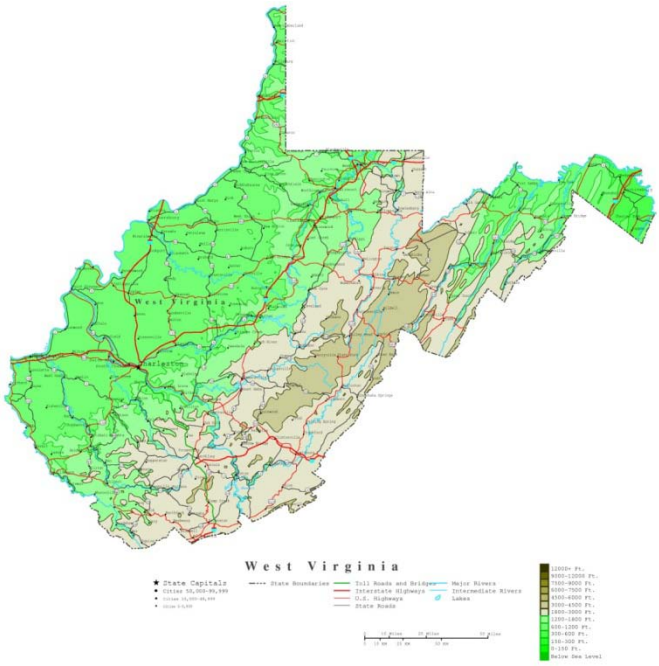

Figure 2: Elevation map of West Virginia [9]

Figure 3 shows the annual wind speed for the state, which increases as you move east [10]. This is due to the higher elevation. The slow turbulent winds of the western part of the state make it the perfect candidate for VAWTs [1].

Although VAWTs are just below horizontal axis wind turbines in average energy production, their power output can be dramatically increased by placing them strategically [2]. A wind farm consisting of only VAWTs may have higher output power per unit of area as opposed to using horizontal axis wind turbines [11].

APPLICATION

To observe the usage of vertical axis wind turbines more practically, the team examined the feasibility of placing turbines at the top of West Virginia University Institute of Technology (WVU Tech) Leonard C. Nelson Engineering Building after reviewing the McKalip and Silman Architects construction plans [12]. When the design was originally created in February 1965, it was determined that height of the building was approximately 28 meters.

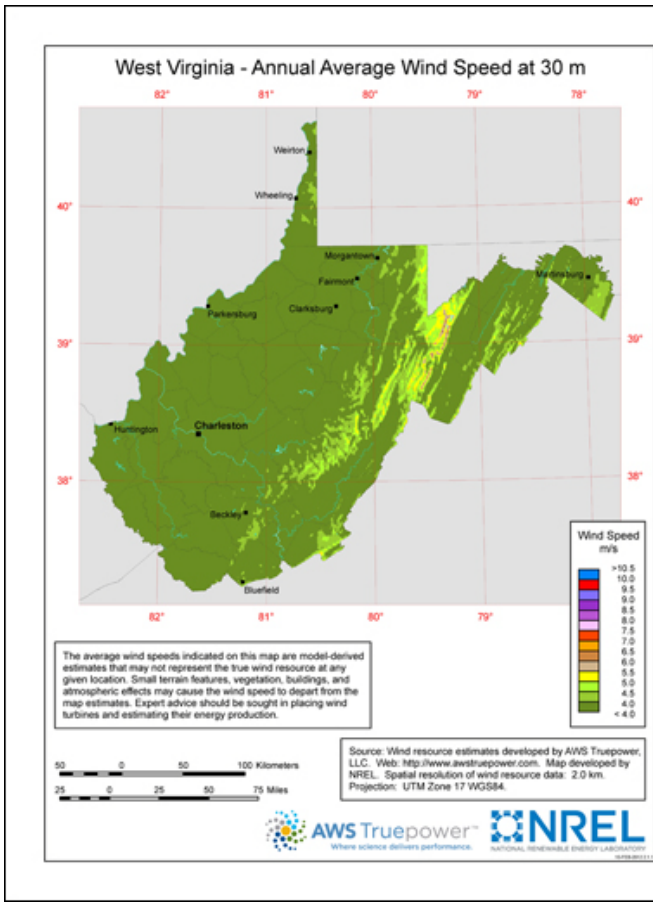

Figure 3: Average yearly wind speed at 30 m in West Virginia [10]

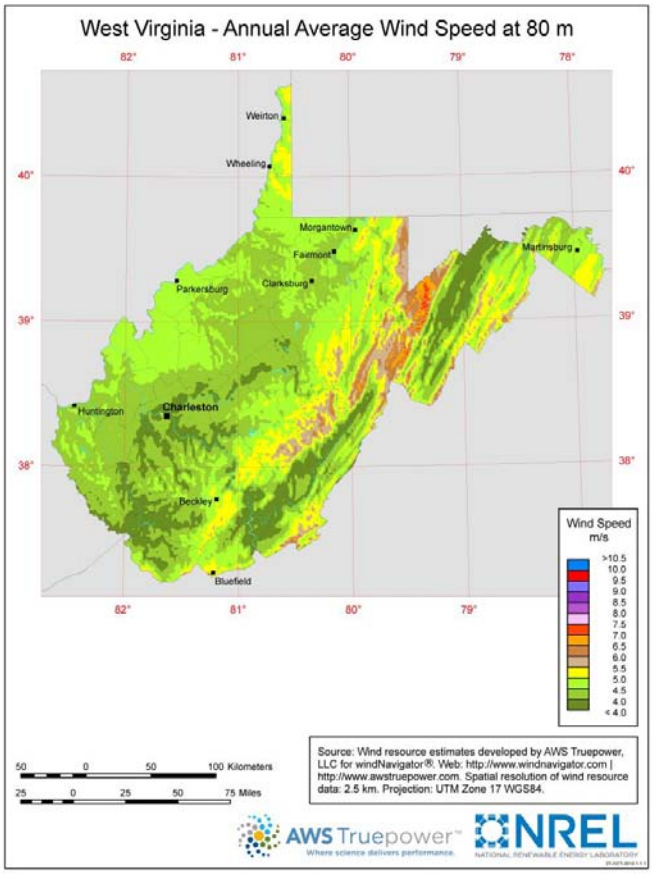

Figure 4: Average yearly wind speed at 80 m in West Virginia [10]

According to Figure 4 the average wind speed for Montgomery, West Virginia wind velocity averages 4.4-5.1 m/s [10]. Figure 4 corresponds to the data collected at the top of the Engineering Classroom Building. Through the usage of a velometer the team measured wind speeds at a variety of angles on all four corners of the building. After evaluating the data, the team determined that the average wind speed was 760 ft/min, which through basic unit conversions is equivalent to 3.9 m/s.

One of the turbine options to use on the Leonard C. Nelson Engineering Building is to use the Solwind quad blade type turbine. Like most vertical axis turbines, the Solwind is extremely quiet [8]. It uses a low speed Magnetic Levitation Alternator Generator [8]. Another benefit of using this type of VAWT in an urban setting is that the mast of the turbine was specifically designed so that it could be installed in remote areas or on top of buildings with ease [8]. The mast of the Solwind turbine also does not require any wires to hold it in place [8]

Another alternative would be the QuietRevolution QR5 VAWT. This turbine is pole mounted (6 meter pole) and is based mostly off of the Darrius design [6]. Based on the specs of the turbine given by QuietRevolution's research website, the turbine produces an annual yield of about 4,197 kWh at 5 m/s [13]. The team used annual yield rate at 5 m/s because it is approximately the wind velocity at the top of the Engineering Building. The generator regulates power at 13.5 m/s, and the turbine cuts off at 26 m/s [13].

Given the data provided, the team examined whether bringing vertical axis wind turbines to WVU Tech would be cost beneficial. After reviewing the data, the team proposed placing one QR5 or Solwind VAWT on top of the Engineering building to power a designated classroom. This "Green Room" will consist of standard energy efficient classroom supplies; the daily power usage is estimated to be 2,340 Watts based on average classroom power use [14].

DISCUSSION

The benefits of VAWTs far outnumber their drawbacks. Because of their better efficiency in rough terrain, they are more ideal for the topographical make-up of West Virginia. VAWTs have relatively high efficiency compared to HAWTs at low wind speeds, meaning that they require less wind to produce energy [5].

Some of the weaknesses of VAWTs are that they can stall in some cases where wind velocity is consistently over 20-30 m/s [5]. In some cases, the central neck may wear quickly because there tend to be a lot of stress exerted on it by the rotors [1].

Future studies need to determine the reliability of VAWTs. As of now, there are limited resources on VAWTs; further studies need to determine what factors contribute to their failure. It also needs to be better determined what needs to be done to prevent them from stalling at low wind speeds. In general, more information needs to become available before companies decide if they want to invest in VAWTs.

After analysis, the team would suggest that West Virginia continue to use horizontal axis wind turbines in their current locations, but create new wind farms in the western part of the state using VAWT technology. With this technology, the state can successfully harness wind power that otherwise would be lost with conventional wind mill designs. Due to varying wind speeds, it would be very difficult to utilize HAWTs in the rough terrain of West Virginia, as they cannot effectively receive wind for multiple directions, which would reduce their output.

Based on the research performed, the team has found it to be circumstantially feasible for VAWTs to be placed at high heights, well above surrounding obstructions in urban and mountainous environments.

CONCLUSION

As West Virginia moves away from fossil fuel energy production, the state has a great opportunity to better utilize its natural resources. Wind can play a critical role in the state's future as a sustainable energy source. Wind mills create the perfect opportunity for the state to meet its energy goals at a low long-term cost [2]. Companies that currently invest in wind technology have taken advantage of West Virginia's high elevations in the eastern part of the state to produce energy thus far, but a new frontier is on the horizon [5].

In the lowlands where wind speeds are slower, the pattern of the wind direction is unpredictable. Wind patterns change by the day if not by the minute [16]. However, using the technology of Vertical Axis Wind Turbines, this wind can now effectively be converted to energy [15]. Here, conventional methods of horizontal axis wind turbines are not profitable [1].

VAWTs offer the possibility to allow West Virginia to utilize more green technology. West Virginia's harsh topography may hinder wind development in the state, but in the future West Virginia will have an opportunity to be at the forefront by properly exploiting what the VAWT design has to offer. Using this technology, the state can successfully create a long term solution to its crucial renewable energy needs [2, 5].

One new method of producing VAWT energy is to harness Virgin territory in the lowlands where wind speed is slower and its patterns are unpredictable.

REFERENCES

[1] "Wind Power--An Illustrated History of Its Development." Wind Power--An Illustrated History of Its Development. N.p., n.d. Web. 23 Sept. 2013. ("Wind Power")

[2] "Wind Energy: A West Virginia Business Opportunity." Wind Energy: A West Virginia Business Opportunity. N.p., n.d. Web. 17 Oct. 2013.

[3] "Innovation in Wind Turbine Design." Google Books.N.p., n.d. Web. 30 Nov. 2013.

[4] Jain, Pramod. "Wind Energy Engineering." Wind Energy Engineering. McGraw Hill, 2011. 72-73. Print.

[5] "Vertical Axis Wind Turbines." WIND-WORKS: Details. N.p., n.d. Web. 30 Nov. 2013.

[6] Francesco Balduzzi, Alessandro, Ennio Antonio Carnevale, Lorenzo Ferrari, Sandro Magnani. "Energy Solutions for a Sustainable World - Proceedings of the Third International Conference on Applied Energy." Applied Energy. Perugia, Italy, 2012. 921-929.

[7] Sandra Eriksson, Hans Bernhoff, Mats Leijon. "Evaluation of different turbine concepts for wind power." Renewable and Sustainable Energy Reviews. 2008. 1419-1434. Print.

[8] Ragheb, m. (2013, April 18). Vertical Axis Wind Turbines. Retrieved from http://mragheb.com: http://mragheb.com/NPRE%20475%20Wind%20Power%20Systems/Vertical%20Axis%20Wind%20Turbines.pdf

[9] "West Virginia Physical Map." And West Virginia Topographic Map. N.p., n.d. Web. 14 Nov. 2013.

[10] "West Virginia 80-Meter Wind Map and Wind Resource Potential." Stakeholder Engagement and Outreach:.N.p., n.d. Web. 17 Oct. 2013.

[11] "SciELO - Scientific Electronic Library Online." SciELO - Scientific Electronic Library Online.N.p., n.d. Web. 01 Dec. 2013

[12] McKalip and Silman Architects, West Virginia University Institute of Technology Leonard C. Nelson Engineering Building Original Blueprint

[13] qr5 turbine details. (n.d.). Retrieved from http://www.quietrevolution.com/: http://www.quietrevolution.com/qr5/qr5-turbine.htm

[14] Anaheim Public Utilities Solar Flag Program: How Much Electricity Does Your Classroom Use? (n.d.). Retrieved from http://anaheimsolarflags.org/: http://anaheimsolarflags.org/solar-power/pdfs/How-Much-Electricity-Does-Your-Classroom-Use-5-20-10.pdf

[15] "West Virginia 50-Meter Wind Map." Wind Powering America:.N.p., n.d. Web. 23 Sept. 2013.(EERE)

[16] "VAWind." VAWind. N.p., n.d. Web. 26 Sept. 2013. (VAWind)

Proceedings of the Fourteenth Annual Early Career Technical Conference
The University of Alabama, Birmingham ECTC 2014
November 1 – 2, 2014 - Birmingham, Alabama USA

DESIGN AND COMMISSIONING OF RENEWABLE RESOURCE POWER GENERATION SYSTEMS AND TESTING PROCEDURES FOR FUTURE RESEARCH CAPABILITIES AT WEST VIRGINIA UNIVERSITY INSTITUTE OF TECHNOLOGY

Garron Ross
Farshid Zabihian
Department of Mechanical Engineering
West Virginia University Institute of Technology
Montgomery, WV, U.S.A.

Asad Davari
Department of Electrical Engineering
West Virginia University Institute of Technology
Montgomery, WV, U.S.A.

ABSTRACT
It is proposed to design and commission a hybrid power generation system utilizing renewable resources by combining solar power with wind power to produce a usable energy source and to facilitate future research at West Virginia University Institute of Technology. The intent of this study is to compare the predicated power output of the system with the actual output values and use this data to discover optimal layout and positioning of the existing equipment. Data will be obtained by developing customized data acquisition programming and testing apparatuses, which will enable further research in the renewable resource power generation field at this campus. Solar and wind power utilization is low in the state of West Virginia due to its mountainous terrain. Maximization of input is necessary if renewable power sources are to be utilized efficiently in this state. With this research and development, it is hoped self-sufficiency at West Virginia University Institute of Technology and the state of West Virginia will become a more feasible reality.

INTRODUCTION
It has been proposed to create a hybrid system utilizing solar radiation and wind that can be used for future research. A testing system is to be designed, programmed, and implemented that would relate weather aspects, including wind speed, wind direction, and solar irradiance, to the power output in Wattage of photovoltaic cells and a wind turbine generator. By comparing the data collected from the test system with theoretical values available in the product specifications of the equipment used, it is hoped to evaluate and assess areas of improvement in conventional PV and wind power systems and potential for new design implementations which are more cost effective, efficient, and improves self –sustainability.

As the global population grows, fewer natural resources will be available. Freshwater supplies are becoming scarcer. Oil will eventually become more difficult to both find and easily and economically extract. However, people can harness the energy of the sun as a renewable resource using photovoltaic cells [1]. The use of solar power is widely used as a core energy source in many nations around the world, but it has some significant disadvantages. Solar power requires large space to maintain power storage during low light times. Improvements in the area are being made using solar mirrors and tracking peak solar irradiance. A wind turbine maintains a much smaller footprint. Solar arrays can also be very expensive and only perform ideally in the particular areas [2, 3].

Graphic 1
U.S. Annual Average Solar Resource

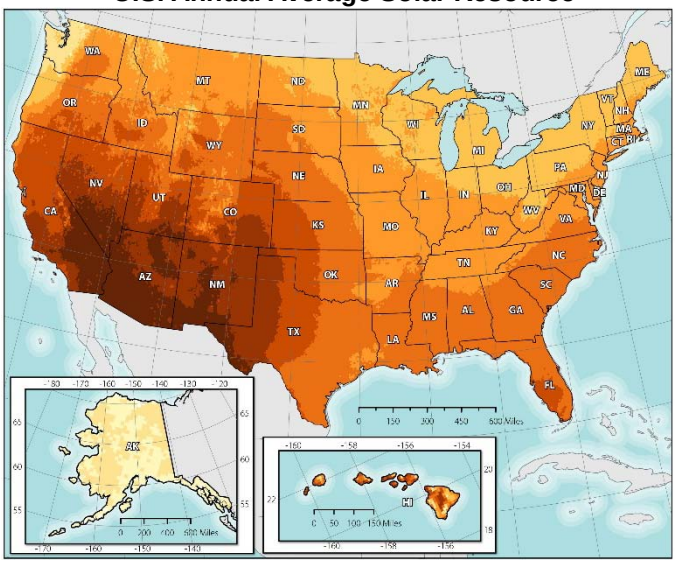

Wind power generation could be more cost effective and a competitive source of energy that can be available globally to anyone; having greater advantages than solar generation. Improvements to maximize efficiency and reduce costs are necessary to make this a reality. Using alternative energy sources can also improve national security, create competition and restrain fossil fuel prices, and help attain energy sustainability [4]. To improve cost effectiveness, a better understanding of potential maximization of existing equipment is necessary. The experimental study discussed in this paper is taking place in an area not recognized as an ideal wind power generation location [5].

Graphic 2
U.S. Annual Average Wind Speed

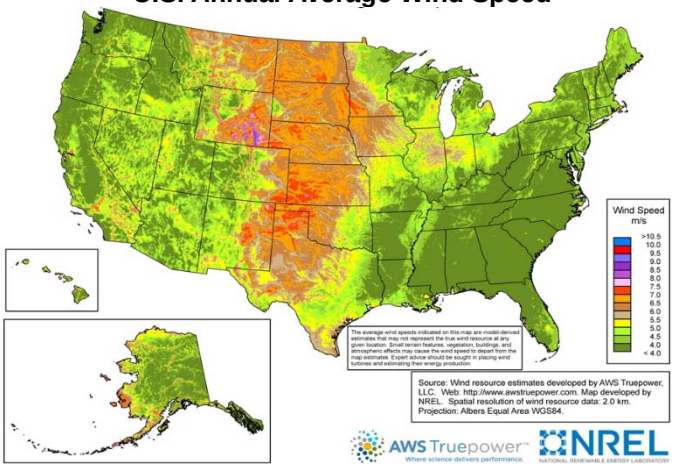

The placement and orientation of the wind turbine is an essential part of the study. Turbulence, vortex shedding, structural interference, etc., are issues to contend with when determining optimal rooftop placement.

NOMENCLATURE

D	Direction
E	voltage, V
G	solar radiation, W/m^2
I	current, A
P	power, W
R	resistance, ohm
T	temperature, K
t	time, h
v	velocity, m/s
Subscripts	
avg	average
PV	photovoltaic
W	wind

EQUIPMENT

The solar array consisted of two Kyocera KC130TM panels rated for 92 W each with a solar irradiance of 800 W/m^2. These panels supply an Outback Power Systems MX-60MPPT charge controller using maximum power point tracking to charge a single 12 V Deka 8A31DT battery. The wind turbine is a roof-mounted Southwest Windpower AirX using 3.81 cm diameter schedule 40 pipe at an elevation of about 1.5 m above the roof surface. The AirX is rated for 400 W at 12.52 m/s and contains an internal charge controller set for 12V. For testing purposes, signal conditioners and voltage transducers were used to detect voltage and current with a DSpace DS1104 module connected by parallel to a PC. MATLAB Simulink and DSpace ControlDesk were used for data acquisition and analysis. After initial testing began, a resistance load was deemed necessary to drain the battery to allow a continuous flow for data consistency. The test configuration is shown in Photos 1 through 4 below.

Photo 1
Existing Solar Array and Wind Turbine

Photo 2
Outback Power Systems Charge Controller

Photo 3
12 V Deka Battery

Photo 4
DSpace Data Acquisition Module

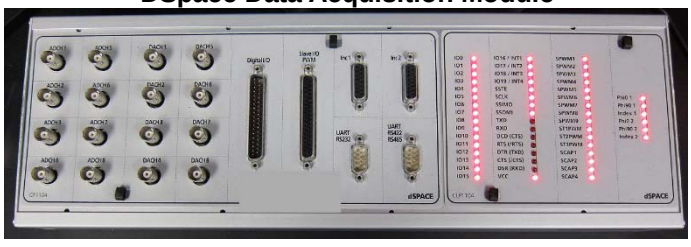

PROCEDURE

Virtual models were created in DSpace ControlDesk and MATLAB Simulink to monitor, calculate, and record data from the hybrid renewable energy system. The model contains defined blocks for collection of voltage and current data through the DS1104 module connected to a PC. Wattage can be calculated through the model internally. Data recording took place through the created program and exported to MATLAB and Microsoft Excel to be analyzed.

With the equipment setup for data recording, experimental tests were conducted to determine positioning of solar array for optimal power output. Extensive measurements of output from the turbine will help determine the feasibility of power production using the AirX turbine in its current position.

The data can be analyzed and compared with theoretical power output, voltage, and amperage values used by the manufacturers of the wind turbine and solar panels tested. Positioning of the panels will be taken into account and related to collected data at each location

RESULTS

Due to the steep learning curve associated with unfamiliar software and limited funding for cost requirements of preferred equipment and software, the team found it difficult to complete the originally proposed tasks. However, work completed has set up the foundation for future research at WVU Institute of Technology in testing alternative energy sources, particularly wind and solar power. The team was capable of creating an application to record basic parameters given the available equipment, including voltage and current.

The output from the existing solar array available was successfully tested. Calculated power output data correlated closely with the manufacturer's specifications given recorded local weather conditions. Fluctuations in the solar panel power output data, were clearly observed due to the MX-60MPPT's preprogrammed settings.

During testing of the wind turbine, an apparent pocket of turbulent airflow surrounding the current location of the wind turbine was observed. The observation was visually made during near ideal conditions specified by the turbine manufacturer in conjunction with local weather reports with limited or no operation and significant shaking and sporadic direction changes. Further difficulties in testing arose due to the connection of the wind turbine and its internal charge controller to the Deka battery and resistance load. Although the manufacturer's recommended wiring schematic was followed, combining the wind turbine and solar array into a hybrid system presented the same testing difficulties provided by the internal charge controller, with the voltage output from the wind turbine matching the battery voltage at any given time.

Samples of power output data were collected using the testing application combining the solar panel and wind turbine power output as a hybrid system. Using voltage and current data from the solar panels and wind turbine, the power output can be calculated. This calculation is completed within the MATLAB model, using the following empirical formula:

$$P = E \times I \qquad \textbf{(1)}$$

Chart 1
PV and Wind V-A Sample

t	E_{PV} (±0.1%)	I_{PV} (±0.5%)	E_W (±0.1%)	I_W (±0.5%)
13:00	31.25	0.70	11.50	0.18
13:15	30.76	0.63	11.33	0.20
13:30	31.37	1.13	11.11	0.31
13:45	31.13	0.94	11.18	0.29
14:00	31.59	0.80	11.18	0.16

Tolerances are indicated for the voltage and current parameters in *Chart 1* as +/-0.1% and +/-0.5%, respectively. These tolerances were specified by the manufacturer of the signal conditioners and voltage transducers used for voltage and current input of the solar panels and wind turbine to the DS1104 module.

Weather data was collected from the nearby weather station, Bee Mountain Station (MBEEW2) in Hernshaw, WV, for comparison between the manufacturer's specifications and the test data [6].

Chart 2
Weather Sample from November 13, 2013

t	*T*	D_W	v_W	G_{ustW}	G_{PV}
13:00	273.75	WSW	3.13	4.92	114.0
13:15	273.75	WSW	3.13	4.92	114.0
13:30	272.05	WSW	3.13	4.92	102.0
13:45	272.05	WSW	1.79	6.26	102.0
14:00	272.05	WSW	1.79	6.26	102.0

Using the power output data collected from Equation *1* and the product function within the MATLAB model, an average power output was calculated by *Equation 2*:

$$P_{avg} = \frac{\sum_{i=1}^{n} P}{n} \quad (2)$$

A P_{avg} of 27.98 W was attained from the sample solar array data collected from 13:00 to 14:00 on November 13, 2013. The G_{avg} calculated using *Equation 2* from *Chart 2* is found to be 106.8 W/m^2. Temperature deration is disregarded with the temperature near 273.15 K [7]. Kyocera states the maximum short-circuit current to be 8.02 A at 1,000 W/m^2 [8]. Therefore, at 106.8 W/m^2 it is expected to measure 0.857 A ideally. The I_{avg} during the specified time frame was found to be 0.896 A giving a percent difference of about 4.5%. The reduction percentage specified by Kyocera is 4.3% for a low irradiance level of 200 W/m^2. Given the test data, the solar array has shown its expected power output during this time of year and is ready for future testing.

Chart 3

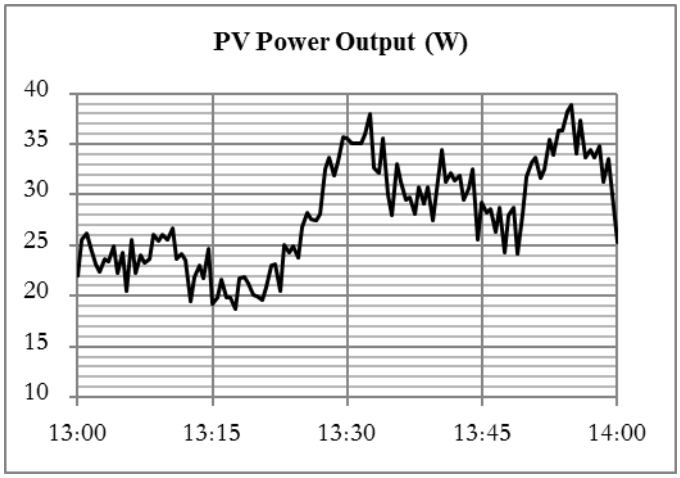

However, the wind turbine has proven difficult to test and testing has provided inconclusive results and requires additional study. The turbine's measurable voltage was nothing more than the voltage of the Deka battery; averaging at 11.22 V. Very little change in measured current occurred and could be attributed to interference between the data acquisition equipment.

Chart 4

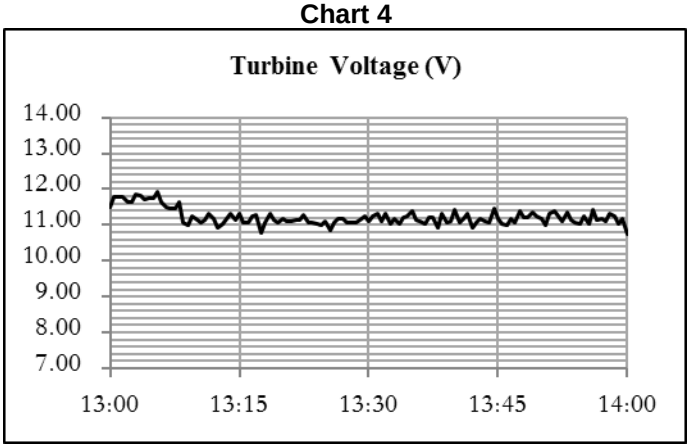

The I_{avg} of the turbine was measured at 0.27 A. Using *Equation 1*; the wind turbine's average power output was calculated to be about 2.97 W across the specified time frame. The AirX specifications indicate a start-up wind speed of 3.60 m/s [9]. As indicated in *Chart 2*, this speed was not attained during the sample collected from 13:00 to 14:00 on November 13, 2013. Further, no significant change in power output was observed during extended additional data collection. The lack of wind turbine operation showed inconclusive results with the existing setup.

DISCUSSION

The ability to test basic attributes of a hybrid power generation system creates a foundation for future applied research at WVU Institute of Technology. Further research and testing equipment is required to evaluate improvements and design potential. Although the wiring layout used for the hybrid power generation system seems to be functional, further research in the layout of test points will allow more accurate testing to take place and would allow testing of other particular variables. Additionally, the use of manufactured charge controllers internally or externally seems to affect performance and test results as they contain preprogrammed responses to power fluctuations and other parameters. This is not conducive to the study of the variables surrounding our power generation system, but works great for simply charging a battery bank for utilization without concern of accurate test data.

The weather data from the Bee Mountain Station seems to provide accurate information and can be used for general solar array analysis but will not provide the data needed for more advanced research in areas such as single or multiple axis solar tracking. The wind data may vary significantly between the weather station and the actual location of the AirX turbine. It is hypothesized that the turbine may be located in a pocket of turbulent airflow over the building to which it is mounted [10, 11]. Testing equipment to measure wind speed and direction is pertinent to the advancement of the authors' study of the turbine's location and analysis of its output.

Graphic 3
Turbulence of Prevailing Wind Over Structures

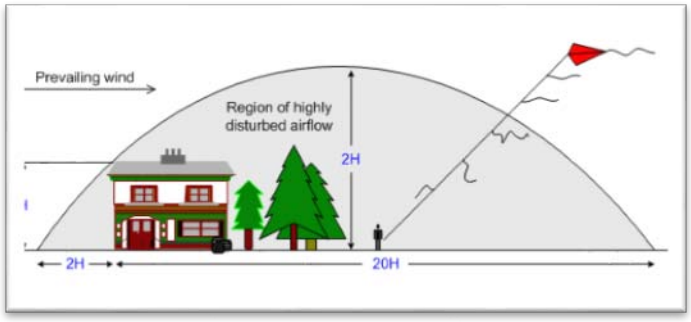

Graphic 4
Airflow Over Roof Edge of Building

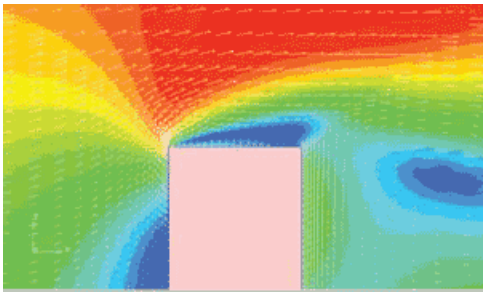

Future plans include the purchase of testing sensors, research of more in-depth testing layouts, and studying the optimal placement and positioning of the components in the hybrid power generation system. Through future research and analysis, it is hoped to determine areas of improvement to maximize power output and utilize the power produced to provide a better roadmap to self-sufficiency.

CONCLUSION

Through this small test project, the team was capable of creating a foundation for future research involving the existing hybrid power generation system. A data acquisition application was created to test and analyze multiple variables surrounding the function of the system. The team has discovered potential paths through the existence of the presented problems for future research utilizing the foundation created during this project.

REFERENCES

[1] United States Department of Energy, 2013, "Photovoltaic Cells," http://www.eere.energy.gov/ basics/renewable_energy/ pv_cells.html

[2] Jordan, D.C., and Kurtz, S.R., 2012, "Photovoltaic Degradation Rates – An Analytical Review," Progress in Photovoltaics: Research and Applications, NREL/JA-5200-51664

[3] National Renewable Energy Laboratory, 2012, "Solar Maps," http://www.nrel.gov/gis/solar.html

[4] Union of Concerned Scientists, 2012, "Why is Renewable Energy Important," http://www.ucsusa.org/clean_energy/res/ aboutwhy.html

[5] National Renewable Energy Laboratory, 2012, "Wind Maps," http://www.nrel.gov/gis/wind/html

[6] Weather Underground, 11/13/2013, "Weather History for MBEEW2,"http://www.wunderground.com/weather WXDailyHistory.asp?ID=MBEEW2&month=11&day=13&year=2013

[7] SMA Solar Technology AG, 2013, "Temperature Derating," files.sma.de/dl/7418/TempDerating-UEN103910.pdf

[8] Kyocera, 2013, "KC130TM – High Efficiency Multicrystal Photovoltaic Module," http://www.kyocerasolar.com/assets/ 001/5186.pdf

[9] Primus Windpower, 2013, "AIR – Owner's Manual," http://www.primuswindpower.com/files/9713/7107/4681/ Primus_Air_Manual_4-2013.pdf

[10] Solacity, Inc., 2013, "Turbine Site Selection," http://www.solacity.com/SiteSelection.htm

[11] Renewable Energy Information Service, 2007, "Urban Challenges: New Research on Integrating Wind Energy in Buildings," http://www.aseanenergy.info/News/34001131.htm

STUDY OF WAVE ENERGY IN THE USA BY DIVIDING AMERICAN COASTS TO SIX REGIONS

Andrew Lytton
Raúl F. Torres
Greg Hawk
Undergraduate Students
Department of Mechanical Engineering
West Virginia University Institute of Technology
Montgomery, WV, U.S.A.

Farshid Zabihian
Department of Mechanical Engineering
West Virginia University Institute of Technology
Montgomery, WV, U.S.A.

ABSTRACT

The main objective of this project is to create an atlas of US coastline for potential wave energy regions. Using the National Data Buoy Center, an estimated value for potential wave energy regions will be calculated in Watts per meter (W/m). This will introduce the idea of energy technologies that can be used to harness wave energy. An atlas of potential wave energy will provide a means to determine which technology is most viable in harnessing energy from waves.

INTRODUCTION

Wave energy is a direct result of wind energy, which forms waves by the following process. Wind hits the surface of the water, causing ripples to form. As ripples form, a larger vertical surface is exposed to the wind. The wind continues to act upon this ripple, causing it to grow larger and larger. The wave will continue to grow in size and power, based on factors such as wind speed, time and distance travelled by the wave.

Water is only a medium that wave energy travels through. This energy is what travels over a long distance, while the water only moves in somewhat of a "rolling" manner.

Several different wave energy converting devices have been proposed, designed, and/or tested. Oscillating Water Columns, Attenuators, Point Absorbers, etc. are a few common families of devices used to convert wave energy. Though each use different processes, some being more complicated than others, each uses a different method to accomplish the same end goal, which is to drive an electric generator.

Purpose

The primary objective of this project is to create an atlas of US coastline for potential wave energy regions. From these regions, some potential areas for wave energy harnessing technology are identified.

Background

Wave energy has a surprisingly old history. The first patent application for wave energy was filed in 1799 [1]. In 1910, the first oscillating water column system was constructed. In the 1970's, interest in alternative forms of energy started to increase due to surging gas prices. As a result, more and more attention has been focused on the application of wave energy. However, up until the 2000's, not many advances were made in the design of a useful unit. That said the field has seen drastic technological changes in the past fifteen years [1].

Theory

The calculation used to obtain the potential wave energy is the power equation, P (W/m) [1],

$$P = \frac{\rho g^2 H^2 T}{32{,}000\,\pi}$$

Where ρ is an average of water density, g is gravitational acceleration, H is calculated as the average of the highest one-third of all wave heights during the 20-minute sampling period and T is the period with maximum wave energy. The buoys record many different types of data including; wind, wave, meteorological, water level, oceanographic, solar radiation, rain, and current. The data used from the buoys was recordings for wave height and average wave period [2, 3].

Procedure

The procedure is relatively basic. Raw data is collected by buoys from "The National Data Buoy Center" [2]. Data from an appropriate buoy is then inserted into an excel file. Unwanted columns not relevant to waves and their potential energy are removed. The relevant data is now filtered to find the square root of the wave height. After the square root of wave height is found, the remaining data is purged to remove any inaccurate results. An average is then taken for the amount of power that is produced per month. While in excel, a macro is used to

organize columns, filter data and to take the square root of wave height.

RESULTS

Observation

The buoys were split up into six regions (Figure 1). Regions 1 and 2 are the northeastern and southeastern Atlantic coast. Region 3 lies in the Gulf of Mexico and regions 4, 5 and 6 are located along the Pacific coast. Results show those regions 1, 2, 4, 5 and 6 yield feasible calculated values for the installation of wave energy harnessing technology. Region 3's lack of complete buoy data rules this region out as a feasible region for energy harnessing technology. However, it is not easy to select one region over another since oceanic and atmospheric conditions are constantly changing. Selecting a region requires a very careful analysis of the data to choose the most efficient and practical location to install wave energy harnessing devices. In making a final judgment as to where these devices would be placed, other local characteristics of each region must be taken under consideration. For example, local maintenance cost, necessity of more renewable energy in the region, and even unique characteristics of the ocean at these locations must be taken into account. The above factors are all going to impact equipment durability and efficiency in the region of choice.

One glaring problem is the lack of information from many buoys surveyed. This issue is evident in each region, but is especially problematic in the Gulf of Mexico. Many of these buoys do not have data, which means the inability to properly analyze the potential for placement of wave energy harnessing devices in the Gulf of Mexico. The Pacific coast seems to be a prime location for placement of these devices around United States coastlines.

Measurements

The following tables and figures were all done with the data collected from National Data Buoy Center and calculations with the power equation.

Figure 1 is a representation of the USA map divided into the 6 regions that were studied.

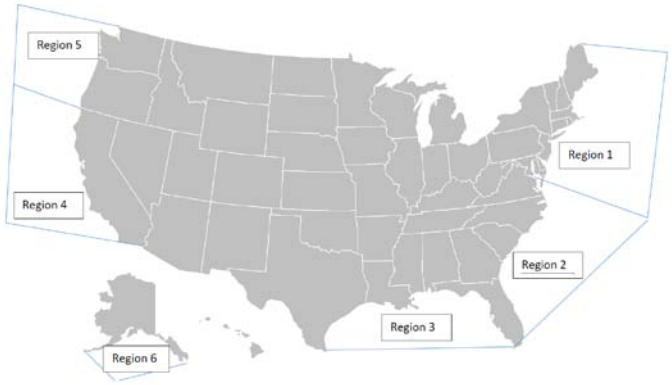

Figure 1. Atlas of USA coastline divided in 6 Regions

For each region certain buoys were selected, not all regions had the same amount of buoys with sufficient data, and there potential wave energy was calculated. The following 7 tables (Table 1- 7) represent these calculations. The tables consist of 3 diferent columns, the first column represents the region and the year it was studied. The last column represents the total wave energy power (W/m) of that region on specific years.The columns between the first and last column show the average wave energy power (W/m) for a staion on the specified year, each station has its own column.

Table 1: Calculated Wave Energy Power for Region 1

Region 1	Station 44005	Station 44007	Station 44027	Station 44037	Station 44098	Station 44013
Year	Watts/meter	Watts/meter	Watts/meter	Watts/meter	Watts/meter	Watts/meter
2013	-	12.18	13.22	38.64	20.8	11.5
2012	18.8	11.57	14.45	27.71	17.84	10.77
2011	22.5	9.61	28.51	25.64	15.18	8.81
2010	30.8	16.63	19.73	-	27.39	18.4

Table 2: Calculated Wave Energy Power for Region 1

Region 1	Station 44097	Station 44065	Station 44009	Station 44066	Total Avg
Year	Watts/meter	Watts/meter	Watts/meter	Watts/meter	Watts/meter
2013	21.79	9.73	14.57	67.5	19.27
2012	22.59	11.68	13.71	80.01	16.86
2011	19.63	10.46	13.6	63.05	18.37
2010	23.87	11.82	17.18	45	22.59

Table 3: Calculated Wave Energy Power for Region 2

Region 2	Station 41014	Station 41036	Station 41004	Station 41008	Station 41114	Total Avg
Year	Watts/meter	Watts/meter	Watts/meter	Watts/meter	Watts/meter	Watts/meter
2013	-	13.57	-	8.23	9.02	10.27
2012	14.98	14.34	11.52	7.54	10.28	11.73
2011	21.36	15.72	15.87	7.59	10.44	14.2
2010	28.52	52.43	13.81	6.74	8.13	21.93

Table 4: Calculated Wave Energy Power for Region 3

Region 3*	Station 42040	Station 42003	Station 42036	Station 42039	Station 42035	Total Avg
Year	Watts/meter	Watts/meter	Watts/meter	Watts/meter	Watts/meter	Watts/meter
2013	12.07	12.11	9.11	12.69	5.79	10.35
2012	9.73	12.78	6.79	8.99	19.35	11.53
2011	9.04	12.07	-	8.81	49.55	19.87
2010	7.02	12	12.71	14.91	29.18	15.16

*Insufficient data in order to determine feasibility

Table 5: Calculated Wave Energy Power for Region 4

Region 4	Station 46213	Station 46207	Station 46232	Station 46214	Station 46239	Station 46205	Total Avg
Year	Watts/meter	Watts/meter	Watts/meter	Watts/meter	Watts/meter	Watts/meter	Watts/meter
2012	92.92	69.88	24.79	91.19	111.64	19.85	68.38
2011	85.43	67.02	22.8	87.33	82.35	14.21	59.86
2010	97.84	85.41	30.53	102.28	83.58	19.81	69.91
2009	73.82	60.35	22.36	83.08	67.04	14.31	53.49

Table 6: Calculated Wave Energy Power for Region 5

Region 5	Station 46089	Station 46229	Station 46041	Station 46211	Station 46015	Station 46087	Total Avg
Year	Watts/meter	Watts/meter	Watts/meter	Watts/meter	Watts/meter	Watts/meter	Watts/meter
2013	67.1	58.85	57.39	50.09	61.06	49.67	57.36
2012	107.1	92.59	76.85	108.32	89.46	53.46	87.96
2011	88.53	80.69	114.75	66.2	58.24	41.14	74.93
2010	107.74	103.01	152.91	81.25	100.52	40.62	97.68

Table 7: Calculated Wave Energy Power for Region 6

Region 6	Station 46001	Station 46076	Station 46077	Station 46060	Station 46078	Station 46075	Total Avg
Year	Watts/meter	Watts/meter	Watts/meter	Watts/meter	Watts/meter	Watts/meter	Watts/meter
2013	82.84	40.16	11.05	4.63	102.82	90.01	55.25
2012	89.49	74.77	12.26	3.85	99.11	96.8	62.71
2011	103.21	43.21	14.89	2.88	107.75	117.58	64.92
2010	92.99	55.94	13.19	7.14	93.86	81.97	57.52

Figure 2 compares the potential wave energy of each region. The wave energy power represented on figure 2 is calculated by averaging the sum of the total averages of wave energy power in each region. As seen on figure 2 region 2 represents the lowest potential wave energy region and region 4 represents the highest potential wave energy region.

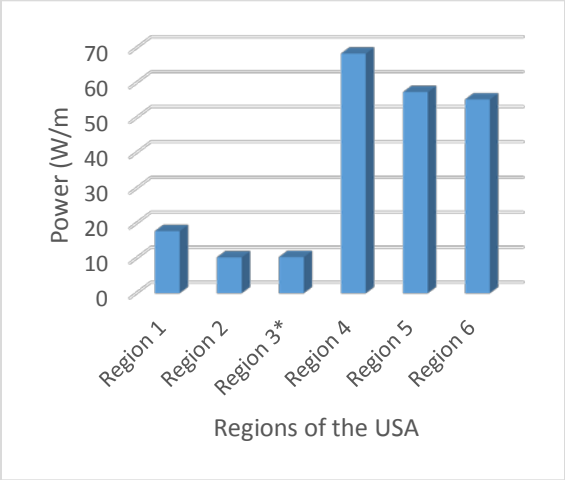

Figure 2. Graphical representation of the Potential Wave Energy per Region

The following tables (table8-12) were made to represent the monthly power averages throughout its specified year. The first column represents the month. The second column represents the potential power generated on the months of the year specified.

Table 8: Calculated Monthly Power Avg. of Region 1

Month:	Year: 2013
Jan	2.46
Feb	6.39
March	16.02
April	-
May	-
June	30.98
July	61.31
August	159.97
September	4.00
October	8.20
November	19.72
December	69.23

Table 9: Calculated Monthly Power Avg. of Region 2

Month:	Year: 2013
Jan	3.75
Feb	6.98
March	10.42
April	12.46
May	16.15
June	16.30
July	15.59
August	12.79
September	16.30
October	17.81
November	16.44
December	17.18

Table 10: Calculated Monthly Power Avg. of Region 4

Month:	Year: 2013
Jan	112.91
Feb	136.83
Mar	97.9
Apr	99.94
May	-
Jun	-
Jul	-
Aug	-
Sep	-
Oct	-
Nov	-
Dec	-

Table 11: Calculated Monthly Power Avg. of Region 5

Month:	Year: 2013
Jan	99.87
Feb	184.5
Mar	69.17
Apr	52.7
May	35.77
Jun	29.68
Jul	25.13
Aug	17.03
Sep	92.82
Oct	56.61
Nov	82.39
Dec	69.54

Table 12: Calculated Monthly Power Avg. of Region 6	
Month:	Year: 2013
Jan	233.5
Feb	128.18
Mar	89.05
Apr	129.95
May	61.23
Jun	61.14
Jul	27.92
Aug	31.11
Sep	62.14
Oct	94.89
Nov	162.34
Dec	160.9

Lastly the following figures (Figures 3 and 4) were plotted to show how the potential wave energy has varied through the year. On each figure the y-axis represents the potential wave energy and the x-axis represents the monthly power averages throughout the year (each color pertains to a specific year).

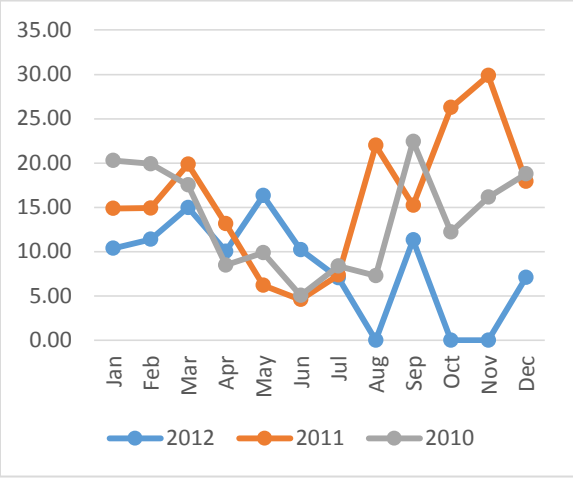

Figure 3. Variation of potential wave energy of Station 41004 (Region 2)

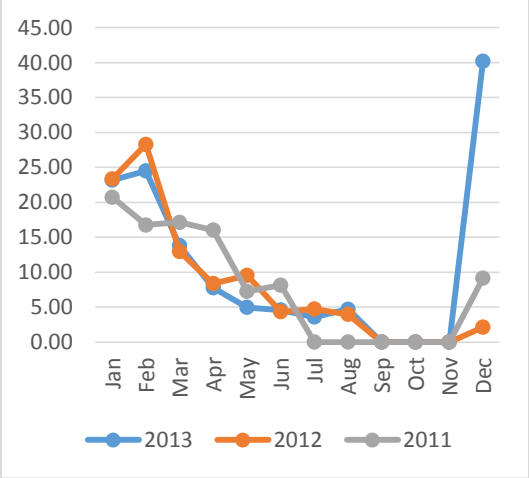

Figure 4. Variation of potential wave energy of Station 41004 (Region 6)

DISCUSSION

In a final analysis of the atlas, results have shown that monthly wave energy is not a completely reliable source of power potential on its own. Major fluctuations in potential power output from month to month are a significant problem. The potential for wave energy is there, and would be a great supplement to the existing power system. However, certain regions are much more practical than others, according to our calculations.

CONCLUSION

The data figures compiled thus far have shown definitive results. A group of experts would certainly be able to use the data to choose an effective and appropriate location to place wave energy converting devices. The fact that the data tables are showing such clear results thus far, in all 3 regions (Atlantic, Gulf, and Pacific), shows that the work is relevant and could be extremely helpful moving forward with wave energy technology.

REFERENCES

1. Zabihian, Farshid. "Review of Marine Renewable Energies: Case Study of Iran." Renewable and Sustainable Energy Reviews (n.d.): n. pag. Print.

2. "National Data Buoy Center." NOAA. N.p., 11 Dec. 2013.<http://www.ndbc.noaa.gov/>.

3. Bowen, Jacon; Fung, Alan; Zabihian, Farshid. “Renewable Wave Energy: A Case Study on the U.S. Coastlines.” June 2-6, 2013.